Mesoscale Convective Complexes over the China during 2005 to 2008

JING XI[1, 2]

(1.Laboratory of Severe Weather, CMA, Beijing, 10081; 2. Shaanxi Yulin meteorological bureau, Shaanxi, Yulin, 719000)

ABSTRACT

Using various synoptic data as satellite image, Doppler radar data and sounding data, we studied 30 MCCs in China occurred between 2005 and 2008. Results indicate that, (1) China MCCs generated mostly between June and August in three regions, Yunnan-Guizhou-Guangdong-Guangxi region, Sichuan region and Huabei(north of China) region. Night is a favorable period for its development, and midnight the best; (2) China MCCs occurred in different background environments, which can be classified different types by lower troposphere, 500 hPa level, and 200 hPa level, its circulation characteristic is outstanding on 200 hPa level; (3) its water vapor is transferred in two ways: direct and indirect; (4) MCC genesis is attended by northern frontogenesis and narrowing processes of spatial high-energy tube; (5) besides, the triggering systems consist of low-vortex shear in lower troposphere coupled with high-value center of θse , the strong divergence at 200hPa level and so on; (6) The tri-dimensional dynamic structure is different between MCC accompanied by precipitation above or beneath torrential rain.

Key words: MCC　China　environmental conditions

1. Introduction

MCC is a meso-α scale convective system recognized from enhanced display of satellite cloud image in 80s of the 20th century. After comprehensively analyzed 10 MCCs in U.S, Maddox defined MCC, and illuminated its structure characteristics at mature stage. Since 2000, Chinese meteorologists have performed relative researches of China MCCs. Jingyu, Jingxi etl, studied MCC induced torrential rain in mid-valley of Huanghe river and Huaihe valley. Lu Yanbin, Yang Benxiang etl, analyzed MCC genesis and development conditions of Huabei plain and regional features of MCCs occurred in the southeast of

Qinghai-Tibet plateau. Kang Fengqin etl, studied vortex, water vapor and heat influx and outflux balance of MCC in south China. Tan Danyu etl, analyzed the physic condition differences between MCCs and cloud clusters generating ordinary torrential rain. In recent years, MCC frequently occurred in Yunnan, Guizhou, Guangdong, Sichuan, and Huaihe valley, usually with torrential rain, strong torrential rain or record torrential rain, which damaged local industry and agriculture. However, predicting MCC-induced rainfall poses a problem to present weather forecast. Neither Japan numerical weather prediction (NWP) model nor T213 NWP model can provide a satisfying prediction result. Hence, it is necessary to perform a in-depth systematic research on China MCC, which could provide useful basis for predicting flood-induced torrential rain triggered by MCC.

2 . Climatic features of China MCC

2.1. Location distribution

In accordance with MCC definition given by document [1], 30 qualified samples were chosen from 2005 through 2008, located in three regions, 16, 54% of the total in Yunnan, Guizhou, Guangxi and Guangdong region (YunGui and LiangGuang region), 7, 23% in Sichuan and neighboring regions, 7, 23% in Henan, Shaanxi, Hebei, and Shandong region (north China region).

2.2. Month distribution

MCCs occurred mostly in 3 months between June and August, in which 17 in June, 8 in July, and 5 in August. June is a high-occurrence month followed by July.

2.3 . Hour distribution

Hourly, the peak period is from 0 to 1 am at mid night. 27% of the total occurred in this period, and 80% from 20：00 pm to next 06：00 am . Night is a favorable period for its occurrence, while mid night appears to be the best.

2.4 . Precipitation intensity

Analyzing maximum precipitation per day induced by MCC, there are 5 record torrential rains, 17% of the total, 15 strong torrential rains, 50% of the total, and 10 stormrains, 33% of the total. In which, 67% exceeded torrential rain.

2.5 . Moving path

China MCCs are stationary in genesis origin.

3. Background environment of MCC development and meso-scale system

3.1. Background environment of MCC development and meso-scale system in YunGui and LiangGuang region

3. 1. 1. 200 hPa-level Circulation and meso-scale system

3.1.1.1. Flow-splitting divergence at synoptic-scale jet exit

Typical sample is shown in Figure 1a. The jet stream axis trends

Nanjiang-Hexizoulang-guanzhong-Henan-Jiangsu. The jet stream widens approximately 10 latitudinal distances. On the right side of the strong wind zone（$V \geqslant 16m \cdot s^{-1}$）, a stream splitting with a big angle(>60°) rotates anti-cyclonically and generates the meso-scale strong divergence area that the divergence reached $2.0 \times 10^{-5}s^{-1}$ (Figure 1b).

3.1.1.2. Flow splitting with strong divergence ahead of short-wave trough

Typical sample is shown in Fig.2a. A trough trending northeast- southwest generated among Yingchuan, Lanzhou, and the east of Tibet plateau, before which was a southwesterly jet trending Hebei-Shanxi-south of Shaanxi-east of Sichuan. In the front of the trough bottom, a flow splitting with big angle rotates anti-cyclonically and generates the strong meso-scale divergence zone that the divergence exceeded $1.2 \times 10^{-5}s^{-1}$ (Fig.2b).

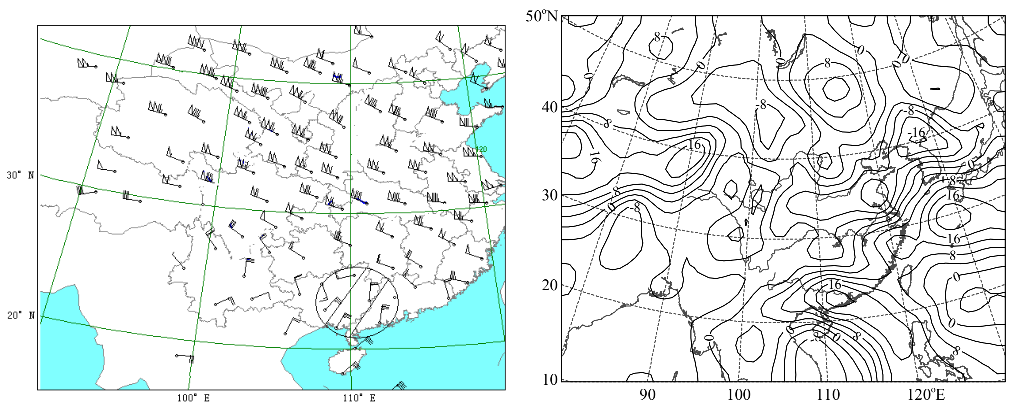

（a） (b)

Fig.1 Wind (a) and Divergence (b) on 200 hPa at 08：00 on 12 June 2005.

Unit：$10^{-6}s^{-1}$(same as followed)

shaded area: developing area of MCC (same as followed)

Solid and dashed line ： shear line or trough line(same as followed)

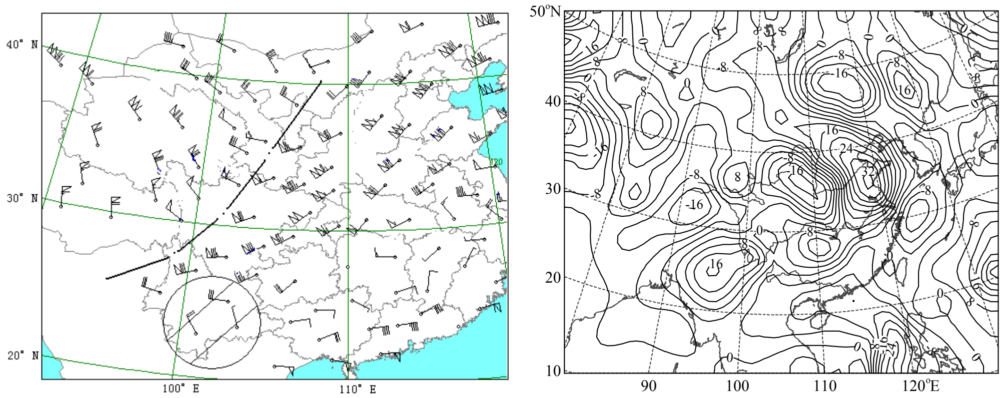

(a) (b)

Fig.2 Wind (a) and Divergence (b) on 200 hPa at 08：00 on 26 June 2005.

3. 1. 2. 500 hPa circulation and meso-scale system

3.1.2.1. The westerly weak trough progresses eastwards and stays stationary

In Fig. 3a, at 20:00 on 11 Jun 2005, a meso-scale weak trough generated to the northwest of MCC genesis region (GR hereafter). At 08:00 on 12 Jun, the trough slightly moved southeastwards and developed(Fig.3b). Meso-scale trough is the direct influencing system of MCC.

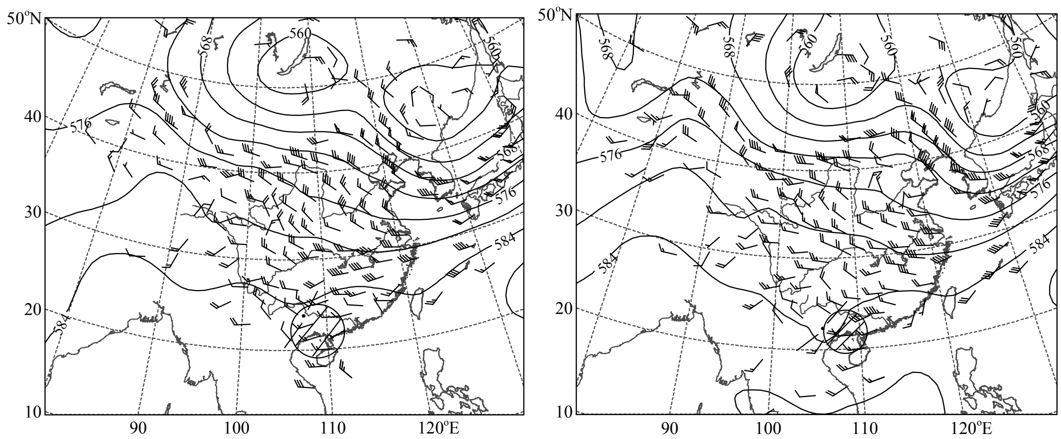

(a) (b)

Fig.3 Height and wind on 500 hPa at 20：00 on 11 June 2005 (a) and at 08：00 on 12 June 2005 (b)
Solid line ： height (same as followed)

3.1.2.2 . Newly-generated weak trough in west southwesterly air flow

As shown in Fig.4a, a west southwesterly stream maintained ahead of the large trough in north of Bengal bay on 500 hPa, to the south of 30° N China. Fig.4b showed that with deepening of India trough, a weak trough generated in Guizhou-Yunnan which triggered genesis of MCC.

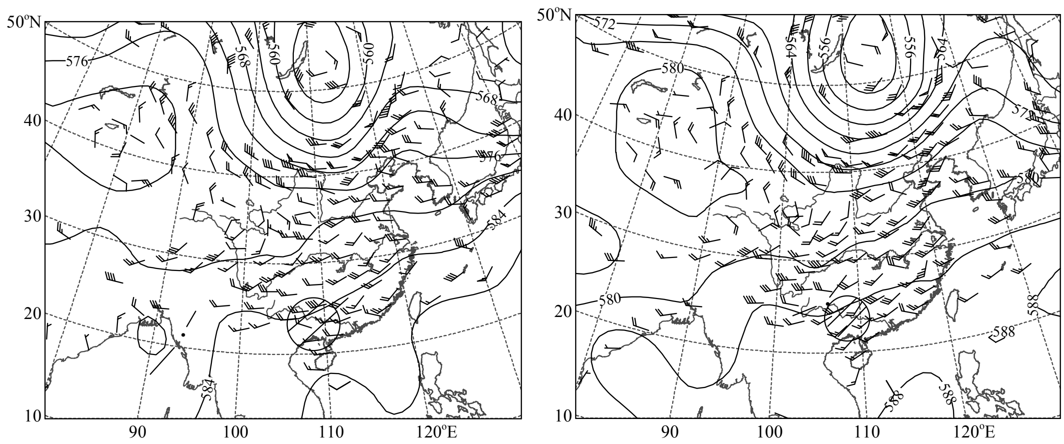

(a) (b)

Fig.4 Height and wind on 500 hPa at 20：00 on 12 June 2006 (a) and at 08：00 on 13 June 2006 (b)

3. 1. 3. Lower-tropospheric circulation and meso-scale system

The influencing systems attending MCC for different region in lower-troposphere are in different levels. 700 hPa is the optimal level for Yunnan MCC, 850 hPa for Guizhou and Sichuan MCC, and 925 hPa or 850 hPa for MCC in Guangxi and Guangdong. The common characteristics of MCC genesis are that the sub-tropical high stays in south of 20° N or east of 110° E. MCC generated in the interacting zone of westerly system and sub-tropical high. In lower troposphere, there are southwesterly or southerly jet stream with a low vortex or stationary shear at its left side.

3.2. Circulation background of Sichuan MCC and meso-scale system

3.2.1. 200 hPa circulation and meso-scale system

Typical sample is shown in Fig.5a. there is a jet axis along Nanjiang-Yinshan trend-Qingdao, at south side of which in east of 90° E was a synoptic scale anti-cyclonical circulation. Sichuan MCC generated in the center of the anti-cyclonical circulation with divergence 1.8× $10^{-5}s^{-1}$(Fig.5b).

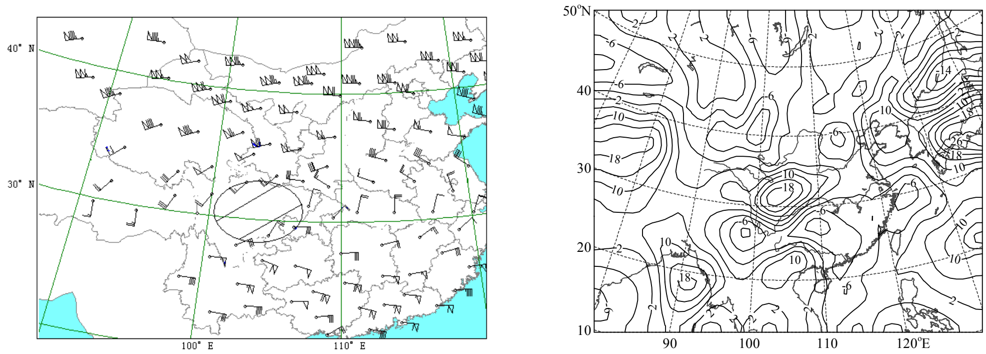

(a) (b)

Fig.5 Wind (a) and Divergence (b) on 200 hPa at 08：00 on 3 July 2005.

3.2.2. 500 hPa circulation and meso-scale system

In Fig.6a, the circulation features high in the east and low in the west in south of 35° N. A northwesterly branch stream from the Tibet plateau near upper reach of Yangtze River at 100° E form a weak trough in Sichuan with a partial southerly flow at the west side of sub-tropical high, which is the direct influencing system of MCC.

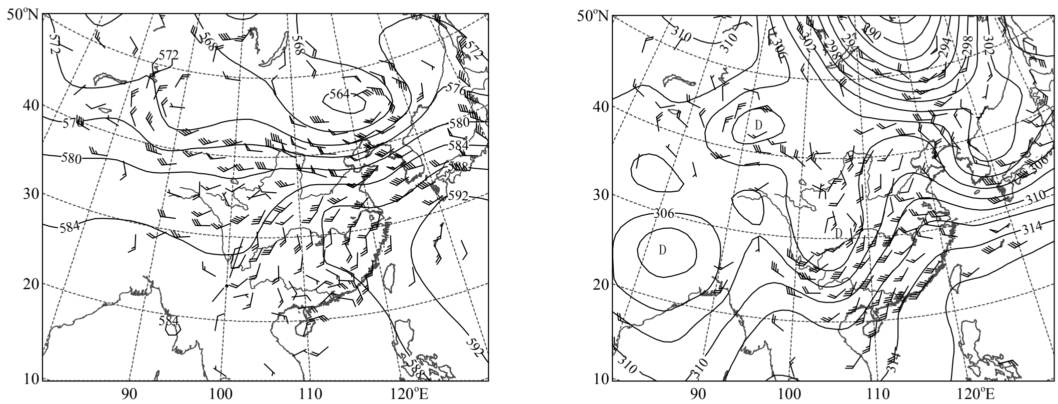

(a) (b)

Fig.6 Height and wind on 500 hPa (a) and 700 hPa (b) at 08：00 on 30 June 2005

3.2.3 . 700 hPa circulation in lower-troposphere and meso-scale system

As shown in Fig.6b, the circulation features high in the east and low in the west in south of 35° N and east of 100° E. A partial southerly or southwesterly jet generated in the east of Sichuan (or southeast of Sichuan to Hunan), at left side of which in the GR generated a meso-α -scale vortex or shear line that triggered genesis of MCC .

3.3. Background environment of MCC development and meso-scale system in north China

3.3.1 . 200 hPa circulation and meso-scale system

3.3.1.1 . Anti-cyclonical circulation develops in front of deep trough

Typical sample shown in Fig.7a, on 200 hPa isobaric surface, a synoptic-scale trough trended Hetao–bordered zone of Gansu and Shaanxi–southeastern Sichuan. A complete meso-α -scale anti-cyclonical circulation generated in front of it with a $1.2\times10^{-5}s^{-1}$ divergence center(Fig.7b), where is the GR of MCC.

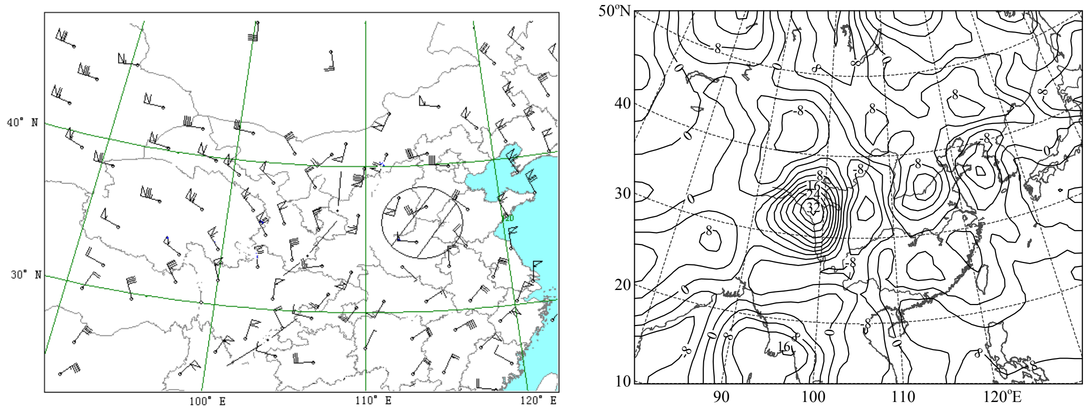

(a) (b)

Fig.7 Wind (a) and Divergence (b) on 200 hPa at 08：00 on 30 July 2007.

3.3.1.2 . Divergence at exit of jet stream

Typical sample shown in Fig.8a, a stream split with big angles at exit of jet stream, which induced a meso-α-scale divergence center in GR with center value >$1.8\times10^{-5}s^{-1}$(fig.8b).

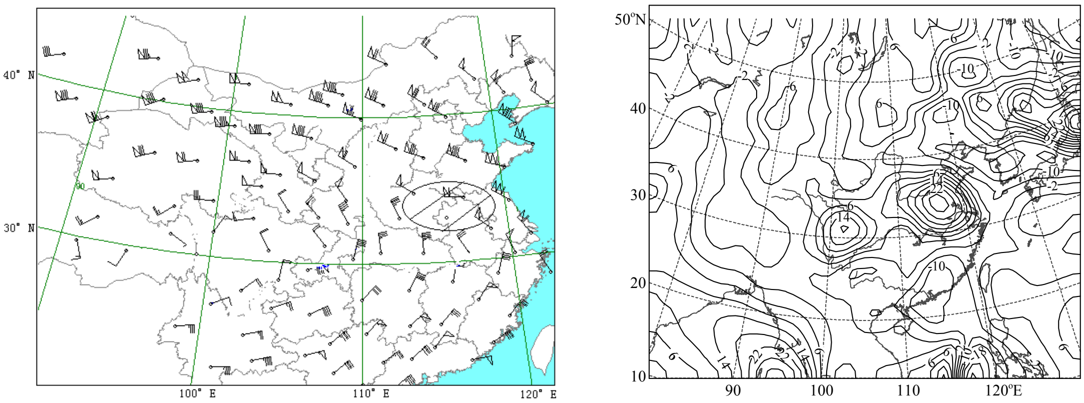

(a) (b)

Fig.8 Wind (a) and Divergence (b) on 200 hPa at 08：00 on 2 July 2006.

3.3.2 . 500 hPa circulation and meso-scale system

3.3.2.1. Weak trough slides in northwesterly stream

As seen in Fig.9a and Fig.9b, a sliding weak trough in front of the Mongolia ridge triggered the MCC genesis and development.

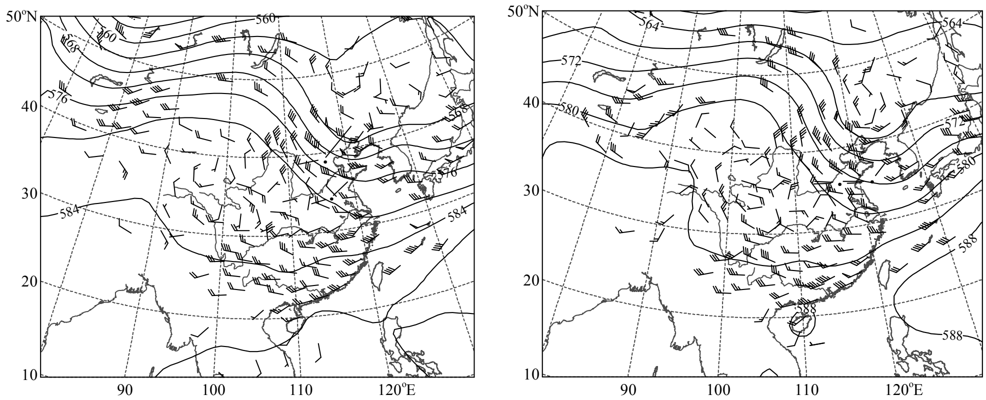

(a) (b)

Fig.9 Height and wind on 500 hPa at 08：00 (a) and 20：00 (b) on 20 June 2005

3.3.2.2. Low vortex development

As shown in Fig.10a, the genesis and development of MCC is accompanied with development of low vortex on 500 hPa level.

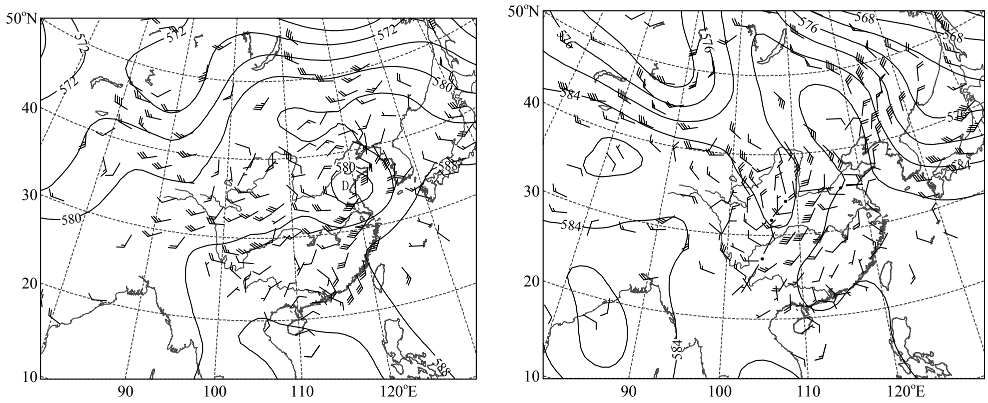

(a) (b)

Fig.10 Height and wind on 500 hPa at 08：00 on 8 August 2005 (a) and at 20：00 on 29 July 2007 (b)

3.3.2.3 . Horizontal shear develops in front of a deep trough

In Fig.10b, MCC developed with the deep trough in Hetao-east of SiChuan. The horizontal shear generated in southwesterly stream in front of the deep trough, where was just the MCC GR.

3.3.3 . Lower-troposphere circulation and meso-scale system

3.3.3.1. 850 hPa-level vortex moves northwards to the MCC

In Fig.11a, on 850 hPa-level isobaric surface, a vortex at west side of the subtropical high moved northwards into the MCC GR, which directly triggered the MCC.

3.3.3.2. Horizontal shear develops before the 925 hPa-level southwesterly or southerly jet stream

Shown in Fig.11b, on 925 hPa isobaric surface, there is a horizontal shear in front of the partial southerly jet at the west side of the subtropical high, which is exactly the triggering system of MCC.

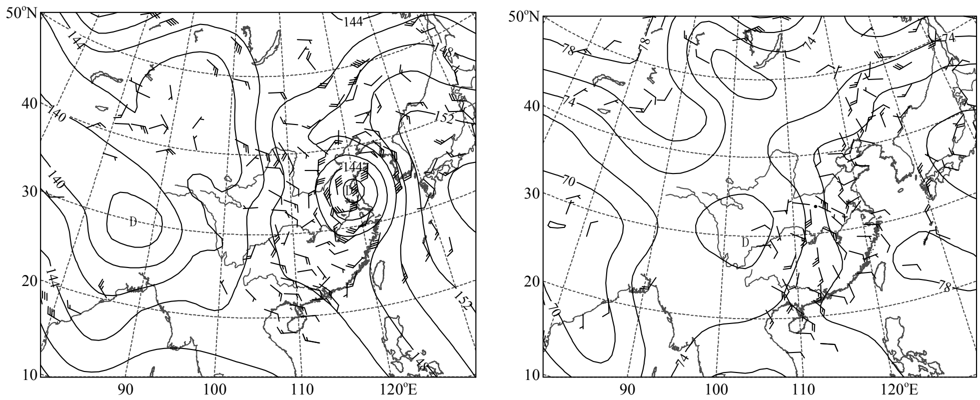

(a) (b)

Fig.11 Height and wind on 850 hPa at 08：00 on 8 August 2005 (a) and on 925 hPa at 20：00 on 29 July 2007 (b)

4. Conditions of MCC genesis

4.1. Water vapor conditions

4.1.1. MCC in Yungui and LiangGuang region

Water vapor is transferred in two ways: direct and indirect in lower troposphere. For direct transfer , water vapor was transferred from the Bengal Bay through indo-china peninsula directly into the MCC GR, and converged in front of the maximum value zone of water vapor flux. For indirect transfer, a maximum value center of water vapor flux appeared in south of the GR accompanied by low-level jet. And water vapor flux converged at left side of the low-level jet where the water vapor flux reached the maximum gradient. On 700 hPa 0r 850 hPa isobaric surface, the water vapor flux of the GR was more than 80 $g \cdot cm^{-1} \cdot hPa^{-1} \cdot s^{-1}$, and normally its convergence $-0.3 \sim -1.2 \times 10^{-7}\ g \cdot cm^{-2} \cdot hPa^{-1} \cdot s^{-1}$. Analysis indicates that the GR corresponds well with the strong divergence center at 200 hPa, and poorly with the low-level water vapor flux center. It is obvious that divergence on 200 hPa level plays a dominating role in MCC genesis and development.

The vertical distribution of the water vapor is also divided in two ways. Firstly, deep moisture, which features the average dew point less than 4.0 ℃ from 850hpa to 200 hPa level. Secondly, dry at upper level and moist at the lower level, which features the average dew point less than 4.0 ℃ from 850hpa to 500 hPa level, and more than 6℃ above 400 hPa level.

4.1.2. Sichuan MCC

The vapor originates from the southern sea, transferred to the east side of the GR by low-level partial southerly jet at the west side of the subtropical high. Between 110 and 120° E on 925 hPa isobaric surface exists a water vapor flux center with maximum value more than 100 $g \cdot cm^{-1} \cdot hPa^{-1} \cdot s^{-1}$. On the same level in the GR generates a converge center of less than -4.6×10^{-7} $g \cdot cm^{-2} \cdot hPa^{-1} \cdot s^{-1}$, which corresponds vertically well with a strong divergence center on 200 hPa level. The vertical distribution is also divided into two types: deep moisture and dry at upper level and moist at the lower level.

4.1.3. North China MCC

Water vapor transfer is also characterized in the basic two ways. Indirectly , the low-level southwesterly jet firstly transfers water vapor to southeast coast to form a high value center of water vapor flux, then , the south wind, a branch of southwesterly jet, carries the water vapor to the GR, where the water vapor flux exceeds $50g \cdot cm^{-1} \cdot hPa^{-1} \cdot s^{-1}$. Directly, the south wind transfers water vapor from east or south China sea to the GR, where the water vapor flux exceeds 50g • cm^{-1} • hPa^{-1} • s^{-1} and its convergence is -0.3～-4.7×10^{-7} g •cm^{-2} •hPa^{-1} •s^{-1}. Analysis indicates that the GR corresponds well with the strong divergence center at 200hpa, and poorly with the low-level water vapor flux center.

4.2. Energy conditions

4.2.1. MCC in Yungui and LiangGuang region

In Fig.12a, before MCC occurrence, a high energy center of $\theta se \geqslant$ 352 K generated on 850 hPa isobaric surface in scope of 10～30 ° N and 90～120° E, in north of which appeared frontogenesis. The uplift dynamic power of frontogenesis triggered the MCC in the converged region. As seen in the cross section of θse along 108 ° E (Fig.12b,Fig.12c), MCC occurs when frontal zone pushed southwards, tilting high–energy tube narrowed, warm advection in lower troposphere maintained and turned to cold advection in upper troposphere, which sustained the instability of the GR. Meanwhile, in lower level of the GR, isoline of θse was evidently steep, according to document[9], which is favorable for the development of tilting vortex in lower troposphere, one of the mechanisms of MCC genesis and development.

Analyzing the convective instability, when the θse difference between 500 hPa and 850 hPa level stays -2～-8 ℃, in most cases, it can be defined as weak convection.

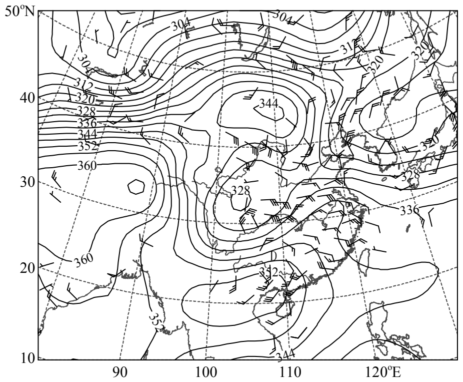

(a)

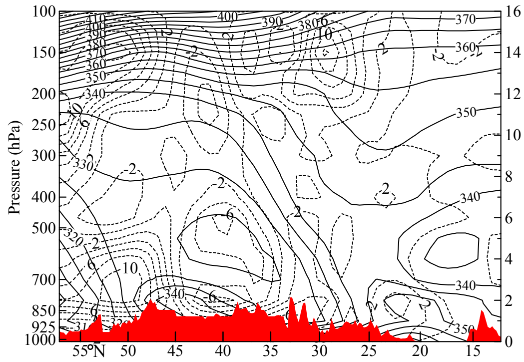

(b)

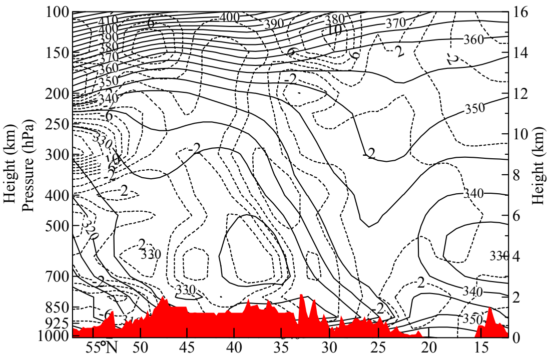

(c)

Fig. 12 θse field on 850 hPa at 20：00 on 8 June 2007. Unit: K(same as followed) (a) and Cross-section diagram of temperature advection and θse along 108° E at 20：00 on 8 June 2007 (b) as well as Cross-section diagram of temperature advection and θse along 108° E at 08：00 on 9 June 2007 (c)

Unit of θse: K(same as followed), Unit of temperature advection： 10^{-4}℃ • s^{-1}(same as followed)

Solid line: θse line(same as followed)

dashed line ： temperature advection line(same as followed)

4.2.2. Sichuan MCC

Take the flood-induced torrential rain case on 3 July 2006, as example. See Fig.13a, at 20:00 on 2 July , on 925 hPa(or 850 hPa) isobaric surface, a high energy center of $\theta se \geqslant 360$ K generated in Sichuan with frontogenesis including northern and western frontogenesis respectively. MCC occurred in the coupled shear line or vortex region of frontogenesis and high energy center. θse difference between 500 hPa and 850 hPa level is between -6～-12 ℃. In Fig.13b and Fig.13c, that the northern low energy region invaded southwards form a high energy tube in GR.

The convective instability of GR was maintained by advance of low energy region in mid-troposphere overlapped high energy region in lower troposphere. The northern frontogenesis triggered instable energy release causing fierce upward motion in the high energy tube, which provides dynamic mechanism for MCC genesis and development.

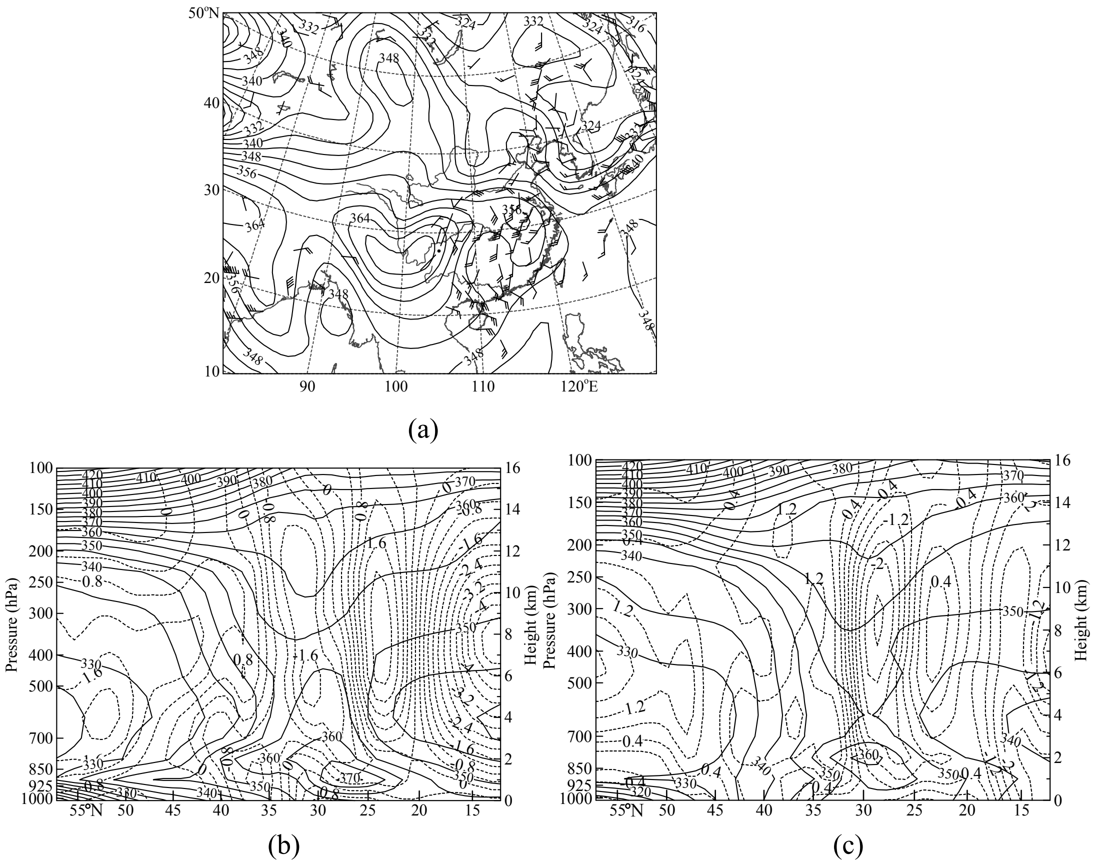

Fig. 13 Wind and θse field on 925 hPa at 20：00 on 2 July 2006 (a) and Cross-section diagram of ω and θse along 102° E at 20：00 on 2 July 2006 (b) as well as Cross-section diagram of ω and θse along 102° E at 08：00 on 3 July 2006 (c)
dashed line ： ω line(same as followed)
Unit of ω： 10^{-3} • hPa^{-1} • s^{-1}(same as followed)

4.2.3. North China MCC

θse difference between 500hpa and 850hpa level is between -7～-14 ℃.

4.2.3.1. “Ω” high-energy system of boundary layer attends northern

frontogenesis

As shown in Fig.14a and Fig.14b, before MCC occurrence, a “Ω” high energy system came into being on boundary layer 925 hPa with center value $\theta se \geqslant 344$ K. MCC was then triggered together with westerly frontogenesis disturbances and shear line’s moving in.

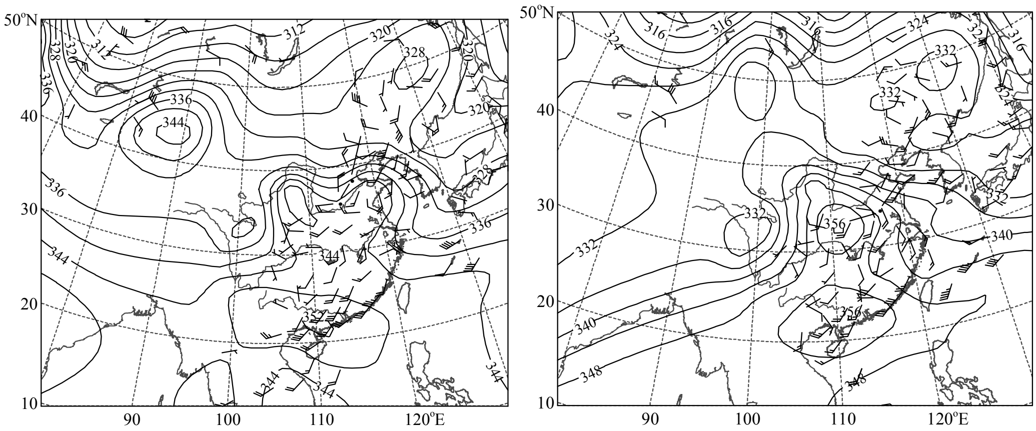

(a) (b)

Fig. 14 Wind and θse field on 925 hPa at 08：00 (a) and 20：00 (b) on 20 June 2005.

4.2.3.2. “Ω” high-energy system of boundary layer attends low vortex

As shown in Fig.15a, with the low vortex coupled with high energy system moving northwards, MCC was triggered in the high energy region with center value $\theta se \geqslant 344$ K.

4.2.3.3. High energy region coupled with horizontal shear line attends western frontogenesis

In Fig.15b, a horizontal shear generated in front of the partial southerly jet coupled with the $\theta se \geqslant 344$ K high energy system, where Frontogenesis from the northwest triggered MCC.

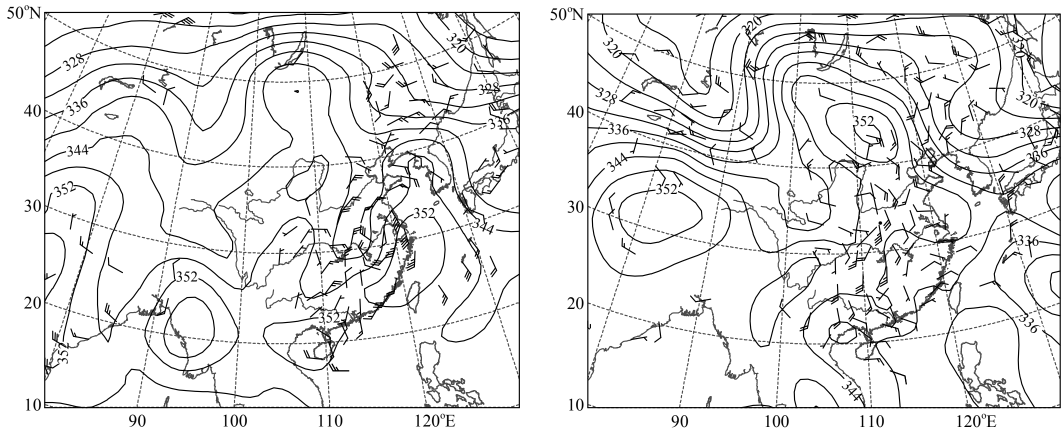

(a) (b)

Fig. 15 Wind and θse field on 925 hPa at 20：00 on 7 August 2005 (a) as well as Wind and θse field on 850 hPa at 20：00 on 29 July 2007 (b)

4.3. Dynamic conditions

4.3.1. Tri-dimensional structure of the dynamic field of MCC caused precipitation above big torrential rain

Fig.16a, Fig.16b and Fig.16c respectively display the tri-dimensional structure of the dynamic field of MCC caused precipitation above big torrential rain. Shown in longitudinal vertical cross section of divergence, there was a deep convergence through lower-mid troposphere in the GR （23 ° N ）, and an evident divergence around 200 hPa level with center value above $18\times10^{-6}s^{-1}$. In related longitudinal vertical cross section of vorticity, there generated a deep, wide (diameter near 1500 km), intensive(vorticity reached $-50\times10^{-6}\ s^{-1}$) negative vorticity region on mid-upper troposphere. Vorticity field coupled with divergence field formed a strong upward-motion column, which built a strong upward motion center with center value below $-2.4\times10^{-3}\cdot hPa^{-1}\cdot s^{-1}$ near 300 hPa level. Obviously, the strong divergence on upper troposphere plays an important role in genesis, development and maintaining of MCC caused precipitation above big torrential rain.

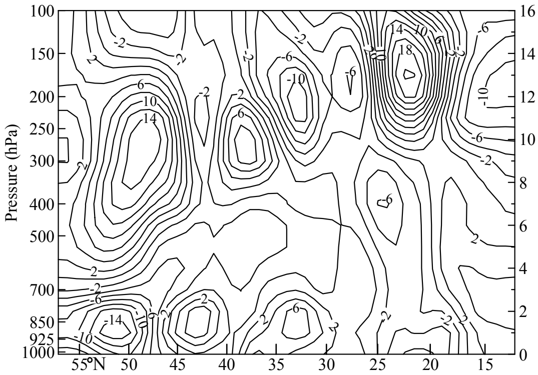

(a)

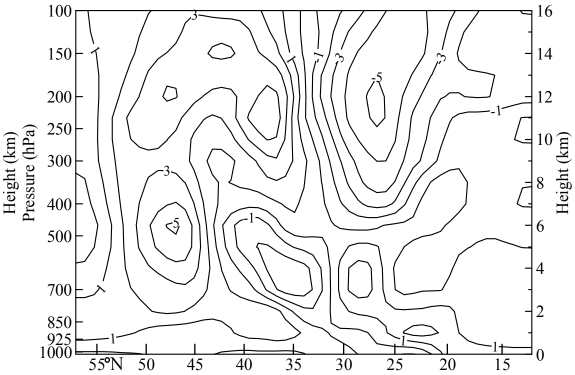

(b)

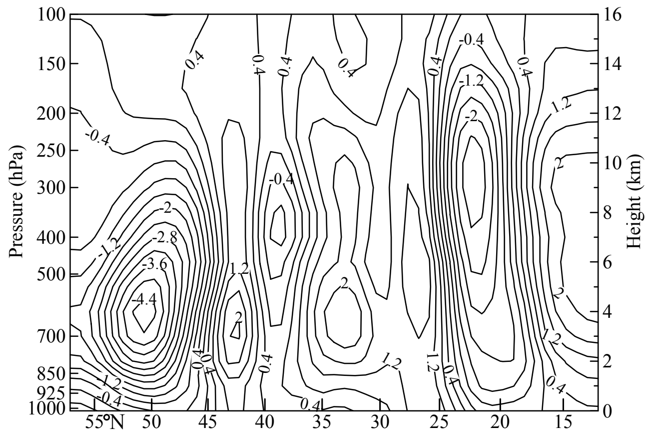

(c)

Fig. 16 Cross-section diagram of divergence (a) , vorticity (Unit: 10^{-6} s^{-1},same as followed)(b) and ω (c) along 110° E at 08：00 on 12 June 2005

4.3.2 Tri-dimensional structure of the dynamic field of MCC caused precipitation below torrential rain

Fig.17a, Fig.17b and Fig.17c respectively display the tri-dimensional structure of the dynamic field of MCC caused precipitation below torrential rain. Shown in longitudinal vertical cross section of divergence, there was a deep convergence through lower-mid troposphere in the GR（25 ° N）, and an evident divergence around 250 hPa level. In related longitudinal vertical cross section of vorticity, there also appeared strong positive vorticity on lower troposphere, but located in the front of positive vorticity center of upper troposphere. Although this match of vorticity and divergence field constructed accordant upward motion in GR, its intensity is much weaker than that of MCC caused precipitation above big torrential rain.

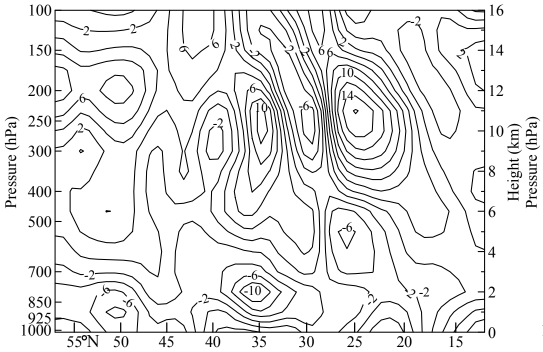

(a)

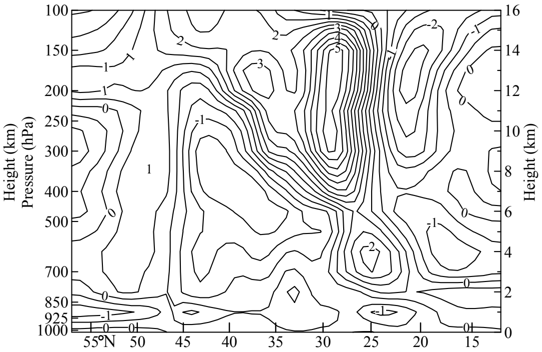

(b)

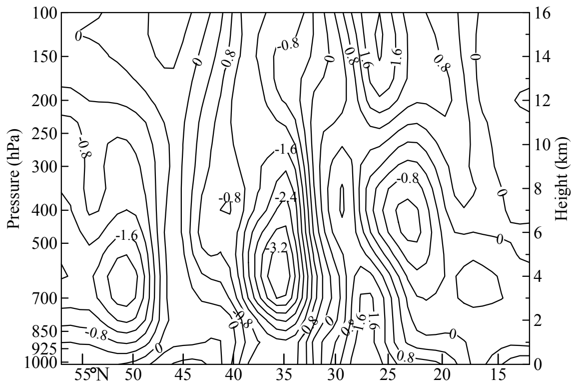

(c)

Fig. 17 Cross-section diagram of divergence (a) , vorticity (b) and ω (c) along 118° E at 08：00 on 26 June 2005

5. Doppler radar echo feature of MCC

5.1. Reflectivity indicates squall line movement inside cloud

Typical case is the MCC induced the big torrential rain event on 8 and 9 Jun 2007, in Guangxi and Guizhou. Characteristics are illuminated in Fig.18 .

Reflectivity and radial velocity evolution show that at 00：04, a portion of MCC has appeared, including tens of meso- γ-scale convective cells. In related velocity field, meso- γ-scale head-wind zone emerged in west southwesterly stream. At 03:00 am, MCC was approaching Radar. On velocity field , southwesterly jet had generated, at left side of which the head wind region enlarged and formed cyclonical convergence. At 04:56 am, a strong convective cloud belt similar to squall line generated at the south edge of the MCC tre nding northeast-southwest with reflectivity⩾45dBz (Fig.18a). On velocity field, a meso- β-scale head wind region emerged in cyclonical region left of the low -level southwesterly jet (negative velocity region). At 07:04 am, the former squall-line-like cloud belt moved east and south of the Radar (Fig.18b), as the velocity field had obvious change . In spite of low-level southwesterly jet's maintaining, 0 velocity region shaped bow in north and 20km south of the radar, and air flow dispersed. 20～200 km south of the radar emerged an anti-cyclonical divergence stream field. A meso- β -scale divergence center with V⩾20 m • s^{-1} formed in upper troposphere. At 08:04 am, the former cloud belt further moved to southeast edge of the radar observation scope and weakened. The velocity field showed maintaining of southwesterly jet and anti-cyclonical divergence field south of the radar, and its center moving to southeast edge of radar observation scope. At 12:01 pm, MCC moved eastwards and weakened . The velocity field exhibited dissipation of southwesterly jet and upper-level divergence center. At 13:00 pm, MCC dissipated .

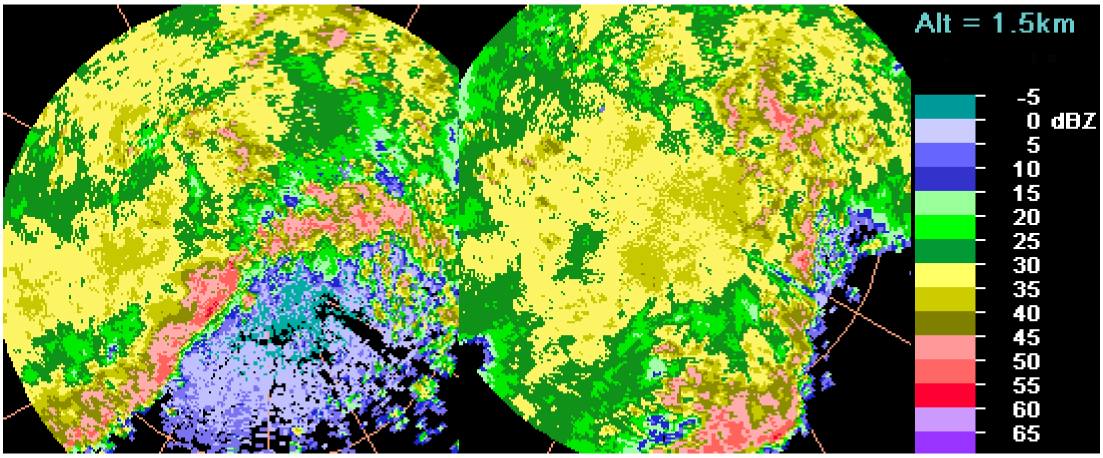

（a）　　　　　　　　　　　　　　　　（b）

Fig. 18 CAPPI(1.5 km) reflectivity images at 04：56（a），07：04（b）on 8 June 2007

5.2. Reflectivity reveals meso-β-scale or meso-γ-scale convective cell development inside cloud cluster.

Typical sample, flood-induced the big torrential rain caused by MCC in middle-reach of Yellow river on 2 July 2006.

At 08:00 am on 2 July, a low-level southeasterly jet generated, at left side of which emerged cyclonical convergence and longitudinal convergence at the same time . The reflectivity illuminated 30 dBZ meso-β-scale cloud cell at the left of the jet (Fig.19a). At 12:01 pm on 2 July (start time of MCC genesis), except expansion of the jet, strong wind belts invaded into the convergence region from southeast and southwest simultaneously. There are scattered small scale divergences on mid-uper troposphere east of radar . The reflectivity showed the cloud cluster enlarged and developed . At 14:01 pm on 2 July, the jet developed, when meso α-scale divergence zone generated on mid-upper level east of radar and the meso-α-scale cloud cluster developed(Fig.19b). at 18:20

pm on 2 July, the mentioned divergence maintained, a $V \geqslant 15\ m \cdot s^{-1}$ jet core generated in the jet . The reflectivity showed the cloud cluster was steady , but on cloud image 1, the cloud cluster developed and enter its mature stage. At 20:06 pm on 2 July, the convergence at left of the jet weakened with inflowing partial south stream. The reflectivity displayed the cloud cluster weakened and turned scattered cloud pieces.

The above analyses indicate that the tri-dimensional structure of the flow field of the big torrential rain caused by MCC is composed of development and maintaining of low-level southeasterly jet, inflowing jet stream at its left side, and its coupling with meso-α-scale divergence zone on mid-upper level.

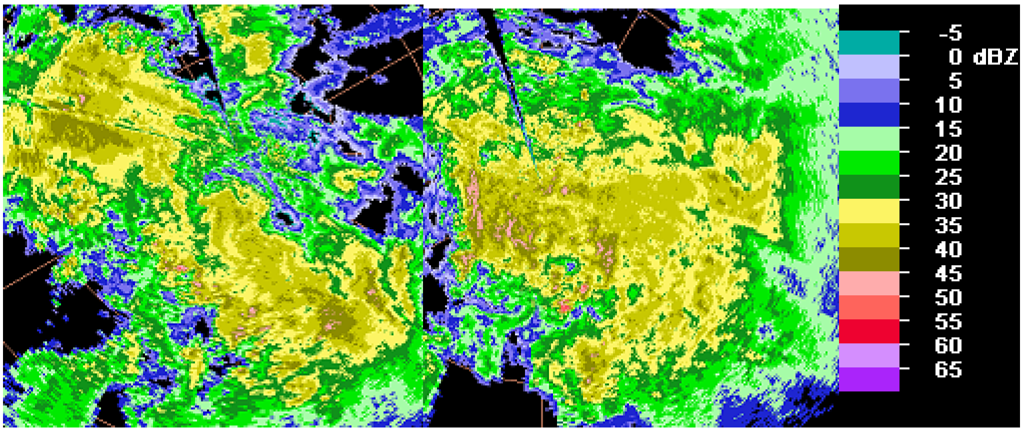

（a） （b）

Fig. 19 2.4° elevation PPI reflectivity images at 08:00（a），14：01（b）on 2 July 2006

6. The main points of forecast of precipitation above big torrential rain caused by MCC

(1) Whether the disposition of the wind field and the divergence field on 200 hPa is advantageous to the MCC genesis and development.

(2) Whether the system's disposition on high and low level is

advantageous to the MCC genesis and development.

(3) Whether the disposition of the wind field and the energy field on 850 hPa or 925 hPa is advantageous to the MCC genesis and development.

(4) Whether the atmospheric stratification is advantageous to the MCC genesis and development.

(5) Whether the Water vapor conditions is advantageous to the MCC genesis and development.

(6) Whether to have the trigger mechanism, such as Frontogenesis, the strong lifting movement developing in upstream and so on.

7. Conclusions

(1) China MCC occurs mainly in the following tree regions: Yungui and Liangguang, Sichuan, and north China, between June and August. Night is a favorable period, mid-night the best. A big portion of China MCC samples are accompanied with precipitation above torrential rain. Meanwhile China MCC is characterized steadily stationary.

(2) China MCC occurs under certain circulation conditions, which is divided into different patterns according to lower troposphere, 500 hPa level, and 200 hPa level. Each pattern has different features.

(3) Water vapor transfer involved in genesis and development of China MCC is classified into two modes: direct and indirect, and its vertical distribution: deep moisture and dry at upper level and moist at the lower level.

(4) before MCC occurrence, θse field forms high value center in the GR. MCC genesis is generally accompanied with northern frontogenesis and narrowing process of spatial high energy tube.

(5)Besides of northern frontogenesis, MCC triggering systems include low vortex shear on lower troposphere coupled with θse high value center, the strong divergence on 200 hPa level and so on.

(6) The tri-dimensional structure of the dynamic field is different between MCC induced precipitation above big torrential rain and below torrential rain.

REFERRENCES

Maddox R A.1980. Mesoscale Convective Complexes.*Bull Am Meteor Soc*,61:1374～1387

Maddox R A.1983.Large-scale meteorological conditions associated with midlatitude mesoscale convective complexes.*Mon Wea Rev*,111:1475～1493

Jingyu, Jingxi, Wangrui,etl. Comprehensive diagnosis of a flood-induced MCC in middle reach of the Yellow river [J].Meteorology，2008，34（3）：56-62

Jingxi, Jingyu, Li Mingjuan, etl. environment and dynamic analysis of a MCC in Huaihe valley [J].Plateau Meteorology，2008，27（2）：349-357

Hou Jianzhong, Sunwei, Dujiwen. Environment and dynamic analysis of a MCC in northeast side of Qinghai-Tibet plateau [J].Plateau Meteorology，2005，24（5）：805-810

Lu Yanbin, Zheng Yongguang, Li Yaping,etl. genesis environment and condition of North China plain [J]. Journal of Applied Meteorology，2002，13（4）：406-412

Liulin, Zhang Guosheng. Several Characteristics of the Environment Field of Mesoscale Convective Complexes over the Northwest of Shandong Province [J].Meteorology，2000，26（11）：40-44

Yang Benxiang，Tao Zuyu. the analysis of local features of MCC on southeast Tibetan Palteau [J].Journal of Meteorology，2005，63（2）：236-242

Kang Fengqin, Xiao Wenan. The Vorticity, Heat, Moisture Budget Evolution of MCC over South China [J]. Plateau Meteorology，2001，20（3）：332-339

Tan Danyu, Jiang Jixi, Fang Zongyi, etl. the differences of synoptic physical condition between MCC and MESO- -scale convective cloud cluster [J]. Journal of Applied Meteorology，2004，15（5）：590-600